Pis'ma v ZhETF, vol. 90, iss. 10, pp. 756 – 760

Electron-phonon interaction in non-polar quantum dots induced by the amorphous polar environment

A. N. Poddubny[1)], *S. V. Goupalov**, *V. I. Kozub*, *I. N. Yassievich*

A.F. Ioffe Physico-Technical Institute, 194021 St. Petersburg, Russia

**Department of Physics, Jackson State University, Jackson, Mississippi 39217, USA*

Submitted 22 October 2009

We propose a Fröhlich-type electron-phonon interaction mechanism for carriers confined in a non-polar quantum dot surrounded by an amorphous polar environment. Carrier transitions under this mechanism are due to their interaction with the oscillating electric field induced by the local vibrations in the surrounding amorphous medium. We estimate the corresponding energy relaxation rate for electrons in Si nanocrystals embedded in a SiO_2 matrix as an example. When the nanocrystal diameter is larger than 4 nm then the gaps between the electron energy levels of size quantization are narrow enough to allow for transitions accompanied by emission of a single local phonon having the energy about 140 meV. In such Si/SiO_2 nanocrystals the relaxation time is in nanosecond range.

PACS: 73.21.La, 73.22.Dj, 78.67.Hc

1. Introduction. The Fröhlich mechanism of electron-phonon coupling is of key importance for carrier energy relaxation in bulk polar semiconductors as well as in heterostructures formed by different polar materials [1 – 7]. One of the examples of such heterostructures is provided by semiconductor quantum dots of *polar* material in a crystalline environment [4, 5]. In this paper we analyze the Fröhlich-like interaction within a *non-polar* inclusion induced by a *polar* amorphous environment. Amorphous media are characterized by a complex vibrational dynamics [8]. In particular, they can possess high-frequency vibrational modes of local (or rather quasi-local) character. These modes are not restricted by any narrow frequency region and can be found with a significant probability at practically any frequency. An extensive review of this problem can be found in Ref. [9]. In this work we will show that the local modes in a polar amorphous medium can induce an alternating electric field even within a non-polar inclusion and thus provide an efficient channel for relaxation of electronic excitations of the inclusion. The proposed mechanism will be discussed as applied to electrons confined in Si nanocrystals in SiO_2, which has recently attracted much attention [10 – 12].

The energy relaxation of an electron confined in a nanocrystal can be induced by high-frequency vibrations of silica glass in the spectral range of 120 meV $\leq \hbar\omega_{\rm ph} \leq$ 160 meV. These vibrational modes have been widely studied by means of molecular dynamics simulations [13 – 16]. In Ref. [16] they were found to be highly localized as their calculated participation ratio exhibited the $1/N$ scaling with the system size, N. [2)]

Although in other simulations substantially higher participation ratios were found, [14] subsequent studies revealed [15] that, even for the high-frequency vibrational modes with relatively large participation ratio, one can always select a small group of atoms oscillating with amplitudes exceeding a certain cutoff. In our model we assign dipole moments to such groups of atoms and introduce the distribution function of the dipole moments in spatial and spectral domains. To demonstrate the proposed mechanism we will focus on the relatively large QDs, where the gaps between the electron energy levels allow the transitions with an emission of only one local phonon of SiO_2.

The rest of the paper is organized as follows. In Sec. 2 we describe a simplified model of a non-polar spherical quantum dot surrounded by a polar environment and derive equations for the time of carrier relaxation induced by local vibrations in the environment. In Sec. 3 we estimate the parameters characterizing local vibrations in a polar glass. In Sec. 4 we present a calculation using the values of parameters describing Si nanocrystals in a SiO_2 matrix. Sec. 5 is reserved for conclusions. Some auxiliary derivations are given in the Appendix.

[1)] e-mail: poddubny@coherent.ioffe.ru

[2)] The crosses and diamonds on Fig.7 of Ref. [16] should be interchanged, as we ascertained from private communication with Dr. C. Oligschleger.

2. Interaction of confined electrons with local vibrations of a polar glass. Let us consider a spherical semiconductor nanocrystal embedded into a polar glass matrix. We will characterize the jth local vibration mode in the glass by the oscillating dipole moment

$$\mathbf{p}_0^{(j)}(t) = \sum_i e_i^{(j)}\,\mathbf{u}_i^{(j)}(t),$$

where $e_i^{(j)}$ and $\mathbf{u}_i^{(j)}(t)$ are the charge and the displacement of the i-th ion participating in the j-th local vibration. The system under study is sketched in Fig.1, where a random orientation of the dipoles is assumed.

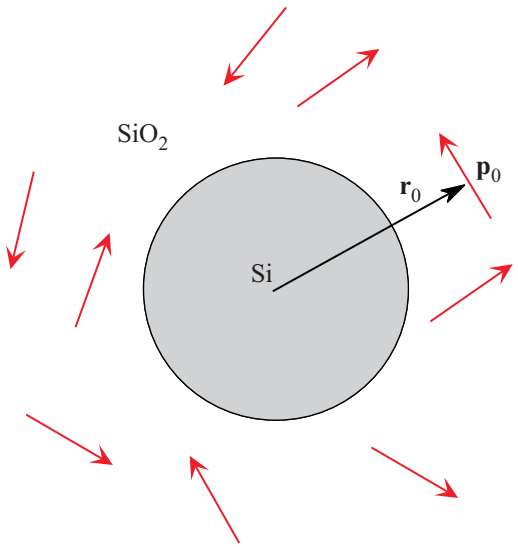

Fig.1. Schematic illustration of the Si QD surrounded by randomly oriented dipoles in SiO_2 matrix. The radius-vector $\mathbf{r_0}$ is shown for one of the dipoles $\mathbf{p_0}$

According to electrostatic approximation (see Appendix) the potential inside the nanocrystal of the radius R and dielectric constant $\varepsilon_{\rm in}$ induced by a point dipole source with polarization $\mathbf{p}_0^{(j)}\delta(\mathbf{r}-\mathbf{r}_0^{(j)})$, positioned in the matrix with dielectric constant $\varepsilon_{\rm out}$, can be represented as

$$e\varphi(r<R,\mathbf{r}_0^{(j)},\mathbf{p}_0^{(j)}) = e\sum_{JM}\alpha_J\frac{r^J}{\left[r_0^{(j)}\right]^{J+2}}\times \\ \times\left[\mathbf{p}_0^{(j)}\cdot\mathbf{Y}_{JM}^{J+1}\left(\mathbf{n}_0^{(j)}\right)\right]^*, \qquad (1)$$

where

$$\alpha_J = \frac{4\pi\sqrt{(J+1)(2J+1)}}{\varepsilon_{\rm in}J+\varepsilon_{\rm out}(J+1)},\quad \mathbf{n}_0^{(j)} = \frac{\mathbf{r}_0^{(j)}}{r_0^{(j)}}. \qquad (2)$$

and $\mathbf{Y}_{JM}^L(\mathbf{n})$ are the vector spherical harmonics introduced in Ref. [17].

We neglect retardation and assume that the different vibration modes are uncorrelated. Thus, the rate of intraband transitions of the electron confined within the spherical nanocrystal under the influence of the quasistatic electric field induced by the local vibrations is given by the Fermi golden rule,

$$\frac{1}{\tau_{\rm loc}} = \frac{2\pi}{\hbar}\sum_j |\langle f|e\varphi(\mathbf{r}_0^{(j)},\mathbf{p}_0^{(j)})|i\rangle|^2\,\delta(E_i-E_f-\hbar\omega_{\rm ph}^{(j)}), \qquad (3)$$

where summation runs over all the local modes of the matrix, E_i and E_f are, respectively, the energies of the initial $|i\rangle$ and the final $|f\rangle$ states of the confined electron.The temperature dependence of the relaxation rate is absent as the energy of phonons emitted $\hbar\omega_{\rm ph}^{(j)} \sim$ ~ 140 meV is much larger than $k_{\rm B}T$ even at room temperatures ($k_{\rm B}$ is the Boltzmann constant). The rather broad distribution of the frequencies of local vibrations allow to satisfy the energy conservation law in Eq. (3). The interaction of electrons confined in a planar quantum layer, where the electron energy spectrum is continuous, with surface phonons at the Si/SiO_2 boundary was considered in Refs. [1, 6, 7]. In case of Si nanocrystals both the electron spectrum and spectrum of surface phonons are discrete and thus the probability to find a granule where the energy conservation law for the process involving the surface phonon mode holds seems to be vanishingly small. Neglecting electron tunneling outside the sphere, one can write the transition matrix element as

$$\langle f|e\varphi(\mathbf{r}_0^{(j)},\mathbf{p}_0^{(j)})|i\rangle = e\sum_{JM}\alpha_J\frac{1}{\left[r_0^{(j)}\right]^{J+2}}\langle f|r^J Y_{JM}|i\rangle\times \\ \times\left[\mathbf{p}_0^{(j)}\cdot\mathbf{Y}_{JM}^{J+1}\left(\mathbf{n}_0^{(j)}\right)\right]^*. \qquad (4)$$

The strength of interaction in (3) decays as a power of r_0. Consequently, the relaxation rate is determined by the interaction not only with the near-surface dipoles $\mathbf{p}_0^{(j)}$, but with a lot of the dipoles located at the distances $r_0 \gtrsim R$ from the QD surface. This character of the interaction makes the relaxation rate insensitive to the microscopic details of Si-SiO_2 interface. It is then reasonable to replace the summation over the different modes in (3) by an integration. We introduce the vibration distribution function as

$$P(\mathbf{r}_0,\mathbf{p}_0,\omega_{\rm ph}) \equiv \mathcal{N}\theta(r_0-R)\times\frac{f(p_0)}{4\pi}\times\rho(\omega_{\rm ph}). \qquad (5)$$

The first factor $\mathcal{N}\theta(r_0-R)$ in (5) describes the uniform distribution of the vibrations in the volume $r_0 > R$ outside the QD with the concentration $\mathcal{N}$. The second factor stands for the isotropic orientation of the

dipoles $\mathbf{p}_0$ in space with the distribution function of the dipole lengthes $f(p_0)$. The last factor $\rho(\omega_{\rm ph})$ in (5) is the distribution function of the vibrations over the frequency. The vibration distribution function can be rigorously obtained only by a sophisticated microscopic calculation. Eq. (5), implying the independence of $\mathbf{r}_0$, $\mathbf{p}_0$ and $\omega_{\rm ph}$, presents the simplest model of the distribution of the dipoles, sufficient for the estimations of the relaxation time presented below. Using the rule $\sum_{(j)} \to \int d\omega_{\rm ph} \int d^3r_0 \int d^3p_0 P(\mathbf{r}_0, \mathbf{p}_0, \omega_{\rm ph})$ we reduce the summation over vibrational modes in Eq. (3) to

$$\frac{1}{\tau_{\rm loc}} = \frac{2\pi}{\hbar}\rho\left(\tfrac{E_i-E_f}{\hbar}\right)\mathcal{N}\int\frac{d^3p_0}{4\pi}f(p_0)\times \times \int\limits_{(r_0>R)} d^3r_0 |\langle f|e\varphi(\mathbf{r}_0,\mathbf{p}_0)|i\rangle|^2. \quad (6)$$

The angular integration can be done with the help of[17]

$$\frac{1}{4\pi}\int d\Omega_{\mathbf{p}_0}\int d\Omega_{\mathbf{r}_0}[\mathbf{p}_0\cdot\mathbf{Y}^{J+1}_{JM}(\Omega_{\mathbf{r}_0})]\times \times [\mathbf{p}_0\cdot\mathbf{Y}^{J'+1}_{J'M'}(\Omega_{\mathbf{r}_0})]^* = \frac{p_0^2}{3}\delta_{JJ'}\delta_{MM'}. \quad (7)$$

Thus, after the averaging over $\mathbf{p}_0$, we get

$$\frac{1}{\tau_{\rm loc}} = \frac{2\pi}{\hbar}\rho\left(\tfrac{E_i-E_f}{\hbar}\right)\mathcal{N}\int_R^\infty dr_0 r_0^2 |\langle f|e\varphi(r_0,\bar{p}_0)|i\rangle|^2, \quad (8)$$

where the matrix element

$$|\langle f|e\varphi(r_0,\bar{p}_0)|i\rangle|^2 \equiv \equiv \int\frac{d^3p_0}{4\pi}f(p_0)\int d\Omega_{\mathbf{r}_0}|\langle f|e\varphi(\mathbf{r}_0,\mathbf{p}_0)|i\rangle|^2 = = \frac{e^2\langle p_0^2\rangle}{3}\sum_{JM}\frac{\alpha_J^2}{r_0^{2J+4}}|\langle f|r^J Y_{JM}|i\rangle|^2 \quad (9)$$

depends only on the length of the vector $r_0 \equiv |\mathbf{r}_0|$ and

$$\langle p_0^2\rangle \equiv \int dp_0 f(p_0) p_0^2. \quad (10)$$

Performing the integration over r_0 we finally obtain

$$\frac{1}{\tau_{\rm loc}} = \frac{2\pi e^2\langle p_0^2\rangle\mathcal{N}}{3\hbar}\rho\left(\tfrac{E_i-E_f}{\hbar}\right)\times \times\sum_{JM}\frac{\alpha_J^2}{2J+1}\frac{1}{R^{2J+1}}|\langle f|r^J Y_{JM}|i\rangle|^2. \quad (11)$$

3. Estimation of the introduced parameters. We need to estimate the mean value of the dipole moment corresponding to a given local vibrational mode. Let us first introduce characteristic values, u and M_0, for the mean square displacement and atomic mass of the atoms participating in the vibration, respectively (we neglect the fact that we deal with different sorts of atoms). This enables us to write

$$\sum_{i=1}^N M_i\langle u_i^{(j)\,2}\rangle\omega_{\rm ph}^{(j)\,2} \sim NM_0u^2\omega_{\rm ph}^2,$$

where N is the number of atoms participating in the vibration, $\omega_{\rm ph} \equiv \omega_{\rm ph}^{(j)}$. At low temperatures

$$NM_0u^2\omega_{\rm ph}^2 \sim \hbar\omega_{\rm ph},$$

and, therefore,

$$u \sim \sqrt{\frac{\hbar}{NM_0\omega_{\rm ph}}}. \quad (12)$$

The dipole moment characterizing this vibrational mode is related to u through

$$\langle p_0\rangle \sim eu\gamma, \quad (13)$$

where the factor γ depends on the relative orientations of displacements for atoms participating in the local mode[3)]. The other glass parameters entering Eq. (11) are the concentration of dipoles, $\mathcal{N}$, and vibrational density of states, ρ. The concentration of dipoles is of the order of

$$\mathcal{N} \sim a^{-3}N^{-1}, \quad (14)$$

where a is the characteristic atomic scale. The rough estimation for the density of states is $\rho \sim 1/(\hbar\omega_{\rm ph})$. Numerical simulations performed for silica glass [14–16] show that the actual phase volume of the high-frequency localized vibrations is at least by a factor of 5 less than the total phase volume. This factor decreases the density of states by about an order of magnitude.

4. Model calculation. In this Section we will perform a model calculation of the relaxation time of electrons confined in relatively large quantum dots where single-phonon transitions are possible. In the simplest case the quantum dot can be treated as a spherical quantum well with the infinite potential barrier. We consider an electron from a simple band with an isotropic effective mass m^* and use the effective mass approximation. In this case the electron states are characterized by the radial quantum number n, the orbital angular momentum l, its projection m onto an arbitrary axis, and a

[3)] In the limiting case when the dipole characterizing a given vibrational mode can be represented as $\sim N$ elementary dipoles oscillating in phase, $\gamma \sim N$. We expect that randomization of phases would lead to $\gamma \sim \sqrt{N}$.

projection of the electron spin. Neglecting for simplicity the electron spin, within the effective mass approximation one can characterize the electron states only by the envelope wave function

$$\psi_{nlm}(\mathbf{r}) = \sqrt{\frac{2}{R^3}} Y_{lm}(\theta,\varphi) \frac{j_l(\varphi_{nl} r/R)}{j_{l+1}(\varphi_{nl})}, \qquad (15)$$

where $j_l(x)$ is the spherical Bessel function, the numbers φ_{nl} are found from

$$j_l(\varphi_{nl}) = 0,$$

and the energy levels

$$E_{nl} = \frac{\hbar^2}{2m^* R^2} \varphi_{nl}^2 \qquad (16)$$

are degenerate over m [18]. Fig.2 shows the dependence of first six energy levels on the nanocrystal diameter,

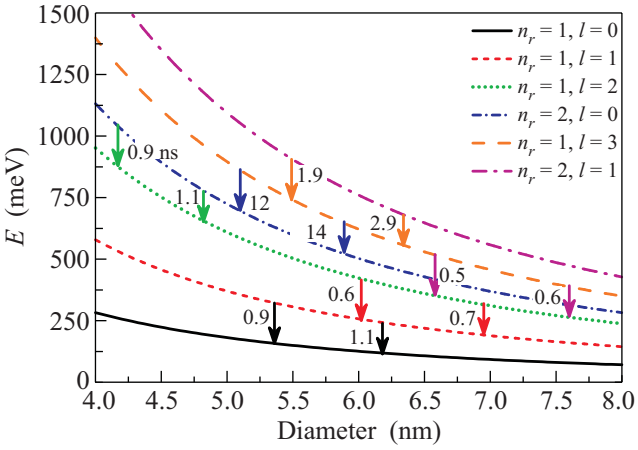

Fig.2. Transition time between the first six energy levels for different diameters of the nanocrystal. The levels are labelled by n_r and l. The transition time values in nanoseconds between the corresponding pairs of levels at given diameter are indicated near the vertical arrows

$2R$, for $2R > 4$ nm, where the value $m^* = 0.33\, m_0$ was used (m_0 is the free electron mass), which corresponds to the density of states mass in Si.

The conduction band of bulk Si has six equivalent minima at the Δ points, and the electron effective mass is strongly anisotropic, $m_{\|} = 0.92 m_0$ and $m_{\perp} = 0.19 m_0$ [19]. This anisotropy leads to the splitting of the energy spectrum (16) for a spherical band, so that additional levels appear in comparison with Fig. 2 [20]. It is also demonstrated in Ref. [20], that the finite barrier for electron tunneling to SiO_2, approximately equal to 3.2 eV [21], shifts down electron levels, which is important for small nanocrystals with diameter $2R < 4$ nm, but the electron density fraction outside the QDs is still less than 0.1. However, for the dots with $2R > 4$ nm the energy levels (16) as a functions of the diameter more accurate calculations [20] for a ground electron state and a number of excited ones. Therefore it is reasonable to apply the simplified model to relaxation time estimation in the considered Si/SiO_2 nanocrystals. A transition between two of the levels of size quantization with the energies (16) is possible when their diameter-dependent difference falls within the spectral range,

$$120 \text{ meV} \lesssim \hbar\omega_{\text{ph}} \lesssim 160 \text{ meV}, \qquad (17)$$

corresponding to high-frequency local vibrations of the silica glass [16]. Vertical arrows in Fig. 2 indicate these allowed regions and the corresponding transition time is shown near each arrow. The calculation is carried out for the set of QD parameters close to that of Si/SiO_2 system: $\varepsilon_{\text{in}} = 12$, $\varepsilon_{\text{out}} = 3$. Our model is too simple to describe the spectral dependence of glass parameters. Thus, we take them at a fixed value in the middle of the range (17), $\hbar\omega_{\text{ph}} = 140$ meV. Other parameters used are as follows: $N = 15$, $\gamma = \sqrt{N}$, $\mathcal{N} = (1/N)\cdot 1.5\cdot 10^{22}\,\text{cm}^{-3}$ and $\rho(\hbar\omega) = 1/(5\hbar\omega_{\text{ph}})$. The vibrating mass, M_0, was taken as $M_0 = (1/3)M_{\text{Si}} + (2/3)M_{\text{O}}$ where M_{Si} and M_{O} are the silicon and oxygen atomic masses, respectively. Since the levels (16) are degenerate over angular momentum projection m, we have summed the relaxation rate (11) over the final states and averaged over initial ones.

Fig. 2 demonstrates that typical value of the relaxation time is of the order of 1 ns. The transition rate is proportional to $1/R$, so it changes with the nanocrystal diameter slower than the energy difference proportional to $1/R^2$.

5. Conclusions. We have shown that interaction of electrons confined in a non-polar quantum dot with local vibrations of amorphous polar environment provides an efficient energy relaxation channel for the "hot" electrons. We have studied as an example the interlevel transitions of electrons confined in Si nanocrystals in SiO_2 matrix with diameters in the range of 4–8 nm, where the transitions proceed through emission of a single local phonon. For such relatively large nanocrystals the values obtained for the transition times are in nanosecond range. Energy relaxation in quantum dots with smaller diameters should be controlled by multiphonon [22] or Auger-like [23] processes.

We are grateful to A.S. Moskalenko for useful discussions. This work was supported in part by the Russian Foundation for Basic Research and by the NSF under Grant # HRD-0833178. A.N.P. also acknowledges the support of the "Dynasty" Foundation-ICFPM.

Appendix.

Let us calculate electric field induced by a point dipole $\mathbf{p}_0$ positioned at the point $\mathbf{r}_0$ outside the sphere of radius R. Dielectric constants inside and outside the sphere are ε_{in} and ε_{out}, respectively. We are interested in the field inside the sphere. Within electrostatic approximation the electric field $\mathbf{E}$ can be expressed via the scalar potential φ as

$$\mathbf{E} = -\operatorname{grad}\varphi. \tag{A1.1}$$

The Poisson equation for the potential φ reads

$$\Delta\varphi = \frac{4\pi}{\varepsilon_{\text{out}}}\operatorname{div}[\mathbf{p}_0\delta(\mathbf{r}-\mathbf{r}_0)] \quad (r_0 > R), \tag{A1.2}$$

and the boundary conditions at the sphere surface are

$$\varphi|_{r=R-0} = \varphi|_{r=R+0}, \quad \varepsilon_{\text{in}}\frac{\partial\varphi}{\partial r}\Big|_{r=R-0} = \varepsilon_{\text{out}}\frac{\partial\varphi}{\partial r}\Big|_{r=R+0}. \tag{A1.3}$$

In the case of a homogeneous medium ($\varepsilon_{\text{in}} = \varepsilon_{\text{out}}$) the solution of (A1.2) is obvious,

$$\varphi_0(\mathbf{r}) = -\frac{1}{\varepsilon_{\text{out}}}\operatorname{div}\frac{\mathbf{p}_0}{|\mathbf{r}-\mathbf{r}_0|}. \tag{A1.4}$$

In what follows it is convenient to use the basis of vector spherical harmonics $\mathbf{Y}^L_{JM}(\theta,\varphi)$ [17]. The identity

$$\frac{\mathbf{p}_0}{|\mathbf{r}-\mathbf{r}_0|} = \sum_{JLM}\frac{4\pi}{2L+1}\frac{r_<^L}{r_>^{L+1}}\mathbf{Y}^L_{JM}(\mathbf{n})[\mathbf{Y}^{L*}_{JM}(\mathbf{n}_0)\cdot\mathbf{p}_0],$$

where $r_> = \max(r,r_0), r_< = \min(r,r_0), \mathbf{n} = \mathbf{r}/r, \mathbf{n}_0 = \mathbf{r}_0/r_0$, is useful to present (A1.4) as a sum of scalar spherical harmonics Y_{JM}. After calculating the derivatives we obtain

$$\varphi_0(\mathbf{r}) = \begin{cases} \sum\limits_{JM}\dfrac{r^J}{r_0^{J+2}}Y_{JM}(\mathbf{n})\xi_{JM}, & r < r_0 \\ \sum\limits_{JM}\dfrac{r_0^{J-1}}{r^{J+1}}Y_{JM}(\mathbf{n})\eta_{JM}, & r > r_0, \end{cases} \tag{A1.5}$$

with

$$\xi_{JM} = \frac{4\pi}{\varepsilon_{\text{out}}}\sqrt{\frac{J+1}{2J+1}}[\mathbf{p}_0\cdot\mathbf{Y}^{J+1}_{JM}(\mathbf{n}_0)]^*,$$
$$\eta_{JM} = \frac{4\pi}{\varepsilon_{\text{out}}}\sqrt{\frac{J}{2J+1}}[\mathbf{p}_0\cdot\mathbf{Y}^{J-1}_{JM}(\mathbf{n}_0)]^*. \tag{A1.6}$$

When $\varepsilon_{\text{in}} \neq \varepsilon_{\text{out}}$ the scalar potential can be written as

$$\varphi(r) = \begin{cases} \sum\limits_{JM} r_{JM}Y_{JM}(\mathbf{n})\dfrac{R^J}{r^{J+1}} + \varphi_0(\mathbf{r}), & (r > R) \\ \sum\limits_{JM} t_{JM}Y_{JM}(\mathbf{n})\dfrac{r^J}{R^{J+1}}, & (r < R) \end{cases}. \tag{A1.7}$$

Substituting (A1.7) and (A1.6) into the boundary conditions (A1.3) we find the coefficients r_{JM} and t_{JM}:

$$t_{JM} = \xi_{JM}\frac{R^{J+1}}{r_0^{J+2}}\frac{(2J+1)\varepsilon_{\text{out}}}{\varepsilon_{\text{in}}J + \varepsilon_{\text{out}}(J+1)},$$
$$r_{JM} = \xi_{JM}\frac{R^{J+1}}{r_0^{J+2}}\frac{J(\varepsilon_{\text{out}}-\varepsilon_{\text{in}})}{\varepsilon_{\text{in}}J + \varepsilon_{\text{out}}(J+1)},$$

which allows to express the scalar potential as (1).

1. K. Hess and P. Vogl, Sol. St. Comm. **30**, 807 (1979).
2. B. K. Ridley, Phys. Rev. B **47**, 4592 (1993).
3. R. Lassnig, Phys. Rev. B **30**, 7132 (1984).
4. M. C. Klein, F. Hache, D. Ricard, and C. Flytzanis, Phys. Rev. B **42**, 11123 (1990).
5. E. Roca, C. Trallero-Giner, and M. Cardona, Phys. Rev. B **49**, 13704 (1994).
6. J.-Q. Lü and F. Koch, Microelectronic Engineering **48**, 95 (1999).
7. M. V. Fischetti, D. A. Neumayer, and E. A. Cartier, J. App. Phys. **90**, 4587 (2001).
8. M. F. Shlesinger, J. Stat. Phys. **36**, 639 (1984).
9. Yu. M. Galperin, V. G. Karpov, and V. I. Kozub, Adv. in Phys. **38**, 669 (1989).
10. A. J. Kenyon, Prog. Quantum Electron. **26**, 225 (2002).
11. L. Pavesi, L. Dal Negro, C. Mazzoleni et al., Nature **408**, 440 (2000).
12. D. Timmerman, I. Izeddin, P. Stallinga et al., Nature Photonics **2**, 105 (2008).
13. Wei Jin, P. Vashishta, R. K. Kalia, and J. P. Rino, Phys. Rev. B **48**, 9359 (1993).
14. S. N. Taraskin and S. R. Elliott, Phys. Rev. B **56**, 8605 (1997).
15. S. N. Taraskin and S. R. Elliott, Phys. Rev. B **59**, 8572 (1999).
16. C. Oligschleger, Phys. Rev. B **60**, 3182 (1999).
17. D. A. Varshalovich, A. N. Moskalev, and V. K. Khersonskii, *Quantum Theory of Angular Momentum*, World Scientific, Singapore, 1988.
18. S. Flügge, *Practical quantum mechanics I*, Springer-Verlag, Berlin – Heidelberg – New-York, 1971.
19. G. L. Bir and G. E. Pikus, *Symmetry and Strain-Induced Effects in Semiconductors*, Wiley, New York 1974.
20. A. S. Moskalenko, J. Berakdar, A. A. Prokofiev, and I. N. Yassievich, Phys. Rev. B **76**, 085427 (2007).
21. S. M. Sze, *Physics of Semiconductor Devices*, Wiley, New York, 1981.
22. T. Inoshita and H. Sakaki, Phys. Rev. B **46**, 7260 (1992).
23. Al. L. Efros, V. A. Kharchenko, and M. Rosen, Solid State Comm. **93**, 281 (1995).